NANO-INDENTATION IN Ti-RICH Ni-Ti SMA AT ROOM TEMPERATURE IN DIFFERENT STRUCTURAL CONDITIONS[1]

Andersan dos Santos Paula[2]
Francisco Manuel Braz Fernandes[3]

Abstract
Their properties and their low cost have made the nickel-titanium (Ni-Ti) shape memory alloys (SMA) attractive in applications where shape memory effect (SME), superelasticity and biocompatibility are important. The goal of the present work is to observe the mechanical behaviour during nano-indentation instrumented test in Ti-Rich Ni-Ti SMA and correlated with shape memory effect. The nano-indentation instrumented test was measured for different structural start conditions (B19' e R-phase) at room temperature. The tests were conducted with different maximum loads: 50, 100, 200, 500 and 1000 mN, with 60 increments on load / unload and 0.5 s between increments. The creep times on maximum load were between 40 and 60 s and for the minimum load was 30 s. According to the structural start condition and maximum load applied it has been possible to correlate the experimental results with the different deformation stage of martensite deformation (elastic deformation, variant reorientation, detwinning, dislocation generation).
Key-words: NiTi shape memory alloy; Mechanical behaviour; Shape memory effect; Nano-indentation.

NANO-INDENTAÇÃO A TEMPERATURA AMBIENTE EM LIGA COM MEMÓRIA DE FORMA DE Ni-Ti RICA EM Ti EM DIFERENTES CONDIÇÕES ESTRUTURAIS

Resumo
Suas propriedades e baixo custo fizeram das ligas com memória de forma de niquel-titânio (Ni-Ti) atrativas nas aplicações onde o efeito de memória de forma (EMF), a superelasticidade e a biocompatibilidade são importantes. O objetivo do presente trabalho é observar o comportamento mecânico durante o teste de nano-identação instrumentada em uma liga com memória de forma de Ni-Ti rica em Ti e correlacionado com o efeito de memória de forma. O teste de nano-indentação instrumentada foi aplicado em diferente condições estruturais iniciais (B19' e fase R) a temperatura ambiente. O teste foi conduzido com diferentes cargas máximas: 50, 100, 200, 500 e 1000 mN, com 60 incrementos no carregamento / descarregamento e 0,5 s entre os incrementos. O tempo de fluência na carga máxima foi de 60 s e na carga mínima foi de 30 s. De acordo com a condição estrutural inicial e carga máxima aplicada foi possível correlacionar os resultados experimentais com os estágios de deformação da martensita (deformação elástica, reorientação das variantes, demaclagem, geração de discordâncias).
Palavras chave: Liga com memória de forma de Ni-Ti; Comportamento mecânico; Efeito de memória de forma; Nano-indentação.

[1] *Contribuição técnica ao 63° Congresso Anual da ABM, 28 de julho a 1° de agosto de 2008, Santos, SP, Brasil*
[2] *D.Sc. and Special Projects Coordinator at Researcher Center of CSN-GGDP/GPD – Brazil*
[3] *D.Sc., Associate Professor at Materials Science Department and Coordinator o Structural Materials Research Group of CENIMAT/I3N, Faculdade de Ciências e Tecnologia, UNL – Portugal*

1 INTRODUCTION

The shape memory alloys (SMA) are very sensitive to changes of the chemical composition and thermal and/or mechanical treatments. The phase transformations responsible for the shape memory effect (SME) in the Ni-Ti SMA are greatly affected by thermal treatments.[1-3] The influences of cold work, annealing and precipitation kinetics during aging on martensitic transformation in the Ni-Ti alloy have been studied by many researchers.[4-6]
According to Antunes et al.,[7] if a sample is composed of several layers (thin films) of different materials on top of a certain substrate, during the nano-indentation test we can infer the mechanical behaviour of those layers and substrate from the analysis of the changes of slopes on plots of log(P) versus log(h). The imposed load will affect in a different way each one of the layers, depending on the total thickness of the layers above the substrate, the indentation depth and the zone deformed by indenter. Based on this behavior, a sample composed of a single phase susceptible to phase changes (B2→B19' or B2→R or R→B19', induced by tension) and/or texture (martensite variants reorientation) can present changes of slopes (that can be associated to those structural changes) when log(P) is plotted versus log(h) from nano-indentation test data [8].
In the present work, the mechanical behavior during nano-indentation instrumented test was studied in Ti-rich (Ni-51.0at.%Ti) Ni-Ti alloy at room temperature in different structural conditions. The phase transformations were analyzed by differential scanning calorimetry (DSC) and phases identified by X-Ray Diffraction (XRD) at room temperature.

2 MATERIALS AND METHODS

The material in study was a Ti-rich Ni-Ti alloy (49.0at.%Ni-51.0at.%Ti, according to SEM/EDS and thickness 2.00 mm) that exhibits shape memory characteristics above room temperature (T_{room}). This alloy was supplied by Memory-Metalle GmbH, Germany (www.memory-metalle.de). According to supplier information, the Ni-Ti alloy was melted in a vacuum induction melting furnace under argon atmosphere, using compact graphite crucibles.

2.1 Samples Conditions

Three samples were analyzed during nano-indentation tests, designated by:

- Sample 1: in as-received (AR) condition was straight annealed by Memory-Metalle GmbH;
- Sample 2: in heat treated (HT) condition was introduced in the furnace at 500ºC during 30 minutes and water quenched;
- Sample 3: in thermalmechanical treated (TMT) condition was subjected to a marforming (cold rolling with 40% thickness reduction) and just after was introduced in the furnace at 400ºC during 30 minutes and water quenched.

2.2 Phase Transformation and Mechanical Behaviour Characterization

Samples with a mass ranging from 40 mg to 50 mg were cut for DSC analysis (SETARAM DSC92). The thermal cycle for the DSC comprised (i) heating up to

180ºC, (ii) holding for 360 s and (iii) subsequent cooling down to -30ºC with heating and cooling rates of 7.5ºC/min.

XRD analysis was performed using a Bruker diffractometer (30 kV/100 mA, rotating anode, CuKα radiation) with conventional θ/2θ coupled scanning at T_{room}.

The Figure 1 shows a schematic diagram representing the critic deformation mechanism that occurs during the indentation.[8] The hardness of Ni-Ti alloy with shape memory can be evaluated by deformation resistance due to the dislocation movement and the martensite formation/reorientation. The area below the unload curve (Figure 1) quantifies the recoverable energy. In Ni-Ti, the deformation energy is recovered by the lattice relaxation (rearrangement of dislocations net or decrease of dislocation density due to subsequent heating) or by reverse transformation. The area between the load and unload curves quantifies the dissipated energy. In Ni-Ti, the energy can be dissipated by the dislocation activity and by the martensite formation/reorientation.

The nano-indentation tests were performed in a Fisher Instrument H100 ultra-microhardness. The tests were conducted with different maximum loads: 50, 100, 200, 500 and 1000 mN, with 60 increments on load / unload and 0.5 s between increments. The creep times on maximum load were between 40 and 60 s and for the minimum load was 30 s.

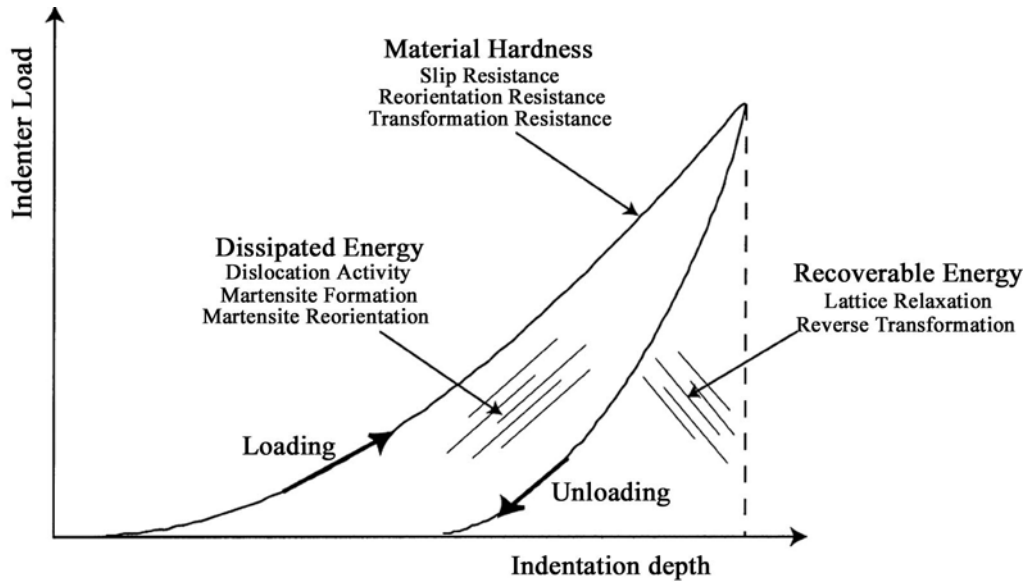

Figure 1 – Schematic diagram showing the critic deformation mechanism that occurs during the indentation. (adapted [8])

The Vickers Hardness calculation from the nano-indentation curves was performed by a program developed in Coimbra University that is described in a Antunes *et al.* [7]

3 RESULTS

Figure 2 shows the thermal characterizations with complete cycles by DSC for the three sample conditions under study: (i) Sample 1 - as-received (AR), (ii) Sample 2 - heat treated in air at 500ºC followed by water quenching (HT), (iii) Sample 3 - cold rolled (marforming) with 35% thickness reduction and subsequent HT. In the Figure 2a on cooling are shown two overlapping exothermic peaks (B2→R; B2→B19' and R→B19') obtained by deconvolution process with CGAS function using "Peak Fitting – Origin 7 software".[9,10]

The transformation temperatures obtained from DSC analysis and transformation sequences are given in Table 1. These values were taken from the kinetics curves calculated by integration of the DSC peaks. [9,10]

Figure 3 shows the XRD spectrum, obtained at T_{room}, for Ni-Ti samples under study.

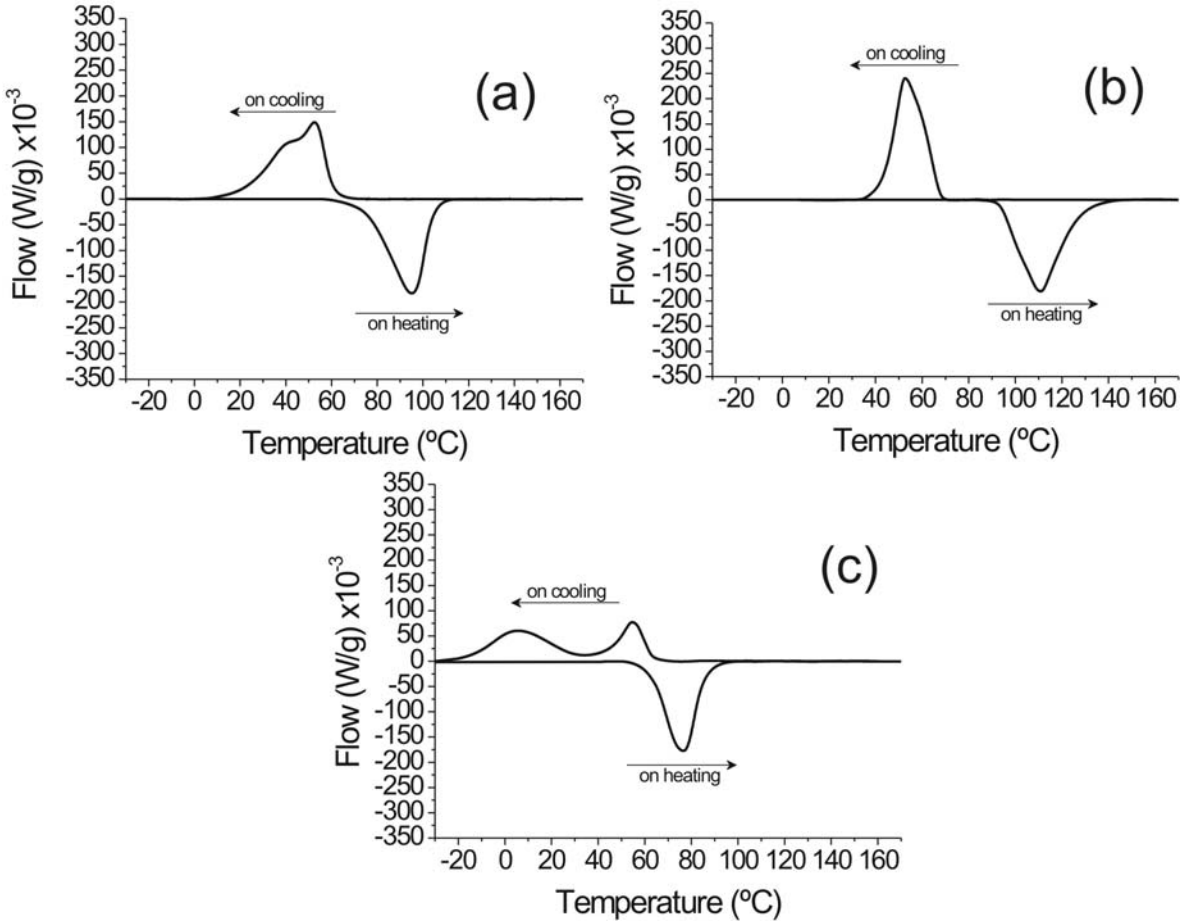

Figure 2 – DSC Curves. (a) Sample 1 – AR condition. (b) Sample 2 – HT condition. (c) Sample 3 – TMT condition.

Table 1 – Sequence and transformation temperatures extracted from DSC analyses.

Structural Condition	Sequences and Transformations Temperatures (ºC)											
	Cooling						Heating					
	B2→R		B2→B19'		R→B19'		B19'→R		B19'→B2		R→B2	
	R_{sc}	R_{fc}	M_s'	M_f'	M_s''	M_f''	R_{sh}	R_{fh}	A_s'	A_f'	A_s''	A_f''
Sample 1	64.9	44.3	58.7	*	*	13.5	66.8	*	*	*	*	106.6
Sample 2	-	-	67.0	35.6	-	-	-	-	94.3	136.0	-	-
Sample 3	63.0	26.0	-	-	26.0	-25.0	-	-	55.0	101.0	-	-

A, R and M refer to the Austenite, Rhombohedral and Martensite phases, respectively. The subscripts s and f refer to the start (1% phase formed) and finish (99% phase formed) temperatures of phase transformations. (-) not detected. (*) not clear.

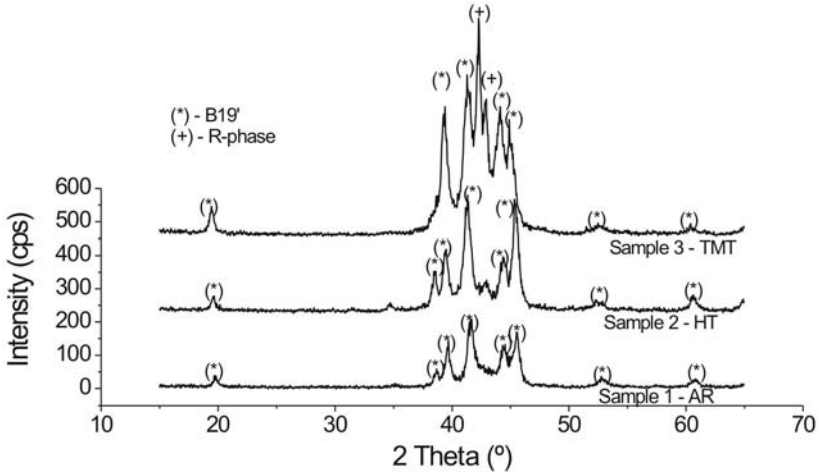

Figure 3 – XRD Spectra for Sample 1 (AR condition), Sample 2 (HT condition) and Sample 3 (TMT condition).

Figures 4, 5 and 6 show the average curve calculated from eight nano-indentation tests (P = 50, 100, 200, 500 e 1000 mN) for Sample 1 (AR), Sample 2 (HT) and Sample 3 (TMT), respectively. According to Figure 2 and 3, for the nano-indentation tests performed at T_{room} Samples 1 and 2 were in B19' field and sample 3, in B19'+R field.

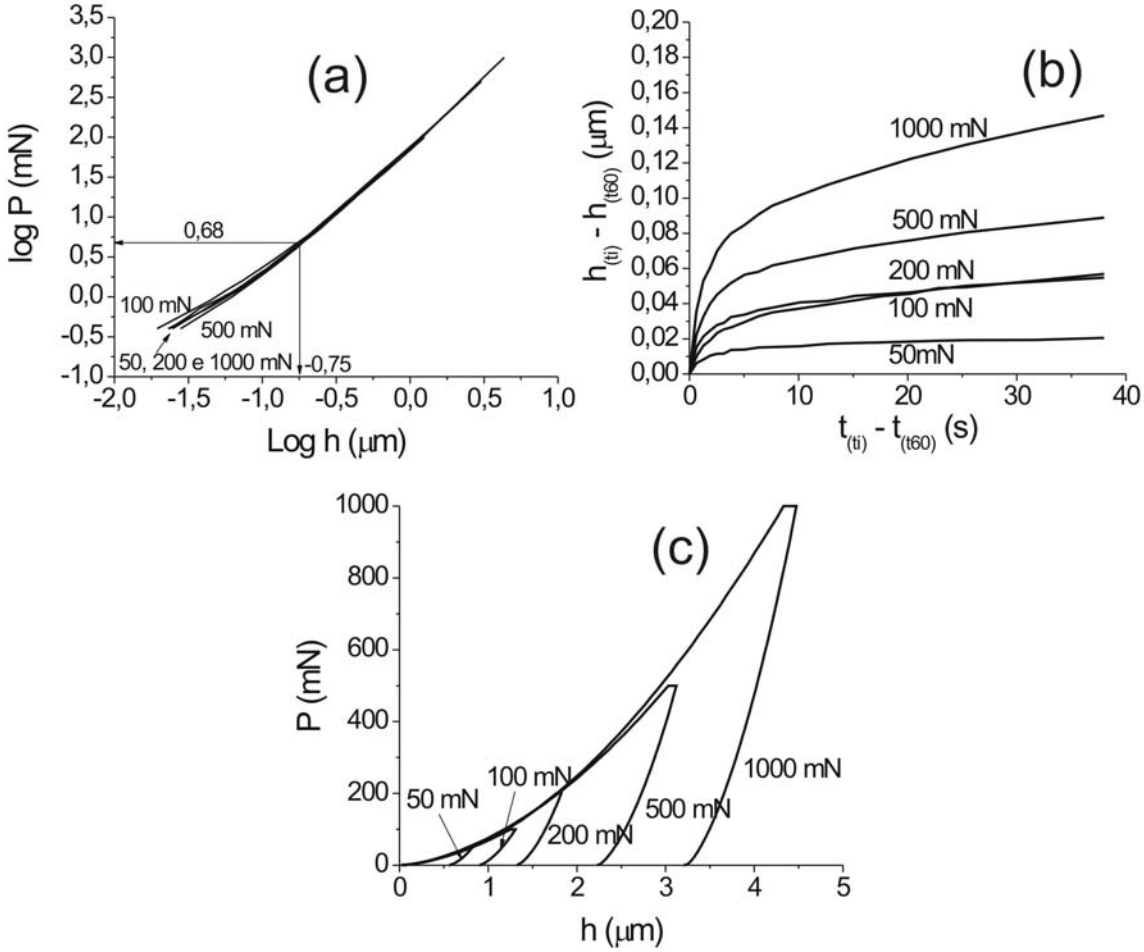

Figure 4 – Nano-indentation Curves for Sample 1 (AR condition). (a) log(P) *versus* log(h) on loading. (b) Depth Stabilization at maximum load. (c) Load (P) *versus* depth (h).

Table 2 shows the values extracted from nano-indentation curves illustrated in this work (Figure 4c, 5c and 6c). These values give the indentation depth at maximum load (h_{max} – μm), the indentation depth after removal of the load (h_f – μm), the dissipation energy (Ed – mN.μm), the recoverable energy (Er – mN.μm), the total energy (E_t – mN.μm) and the Vickers Hardness (HV).

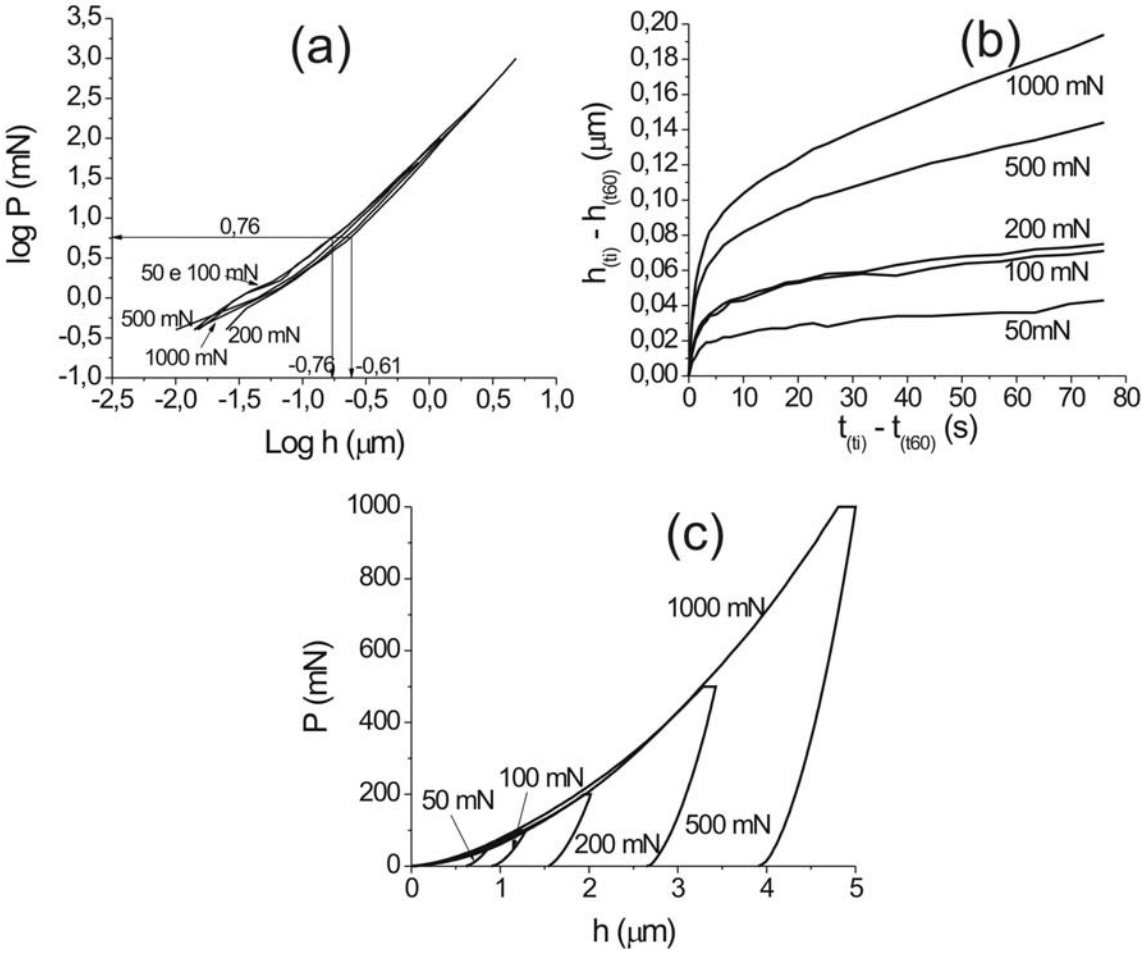

Figure 5 – Nano-indentation Curves for Sample 2 (HT condition). (a) log(P) *versus* log(h) on loading. (b) Depth Stabilization at maximum load. (c) Load (P) *versus* depth (h).

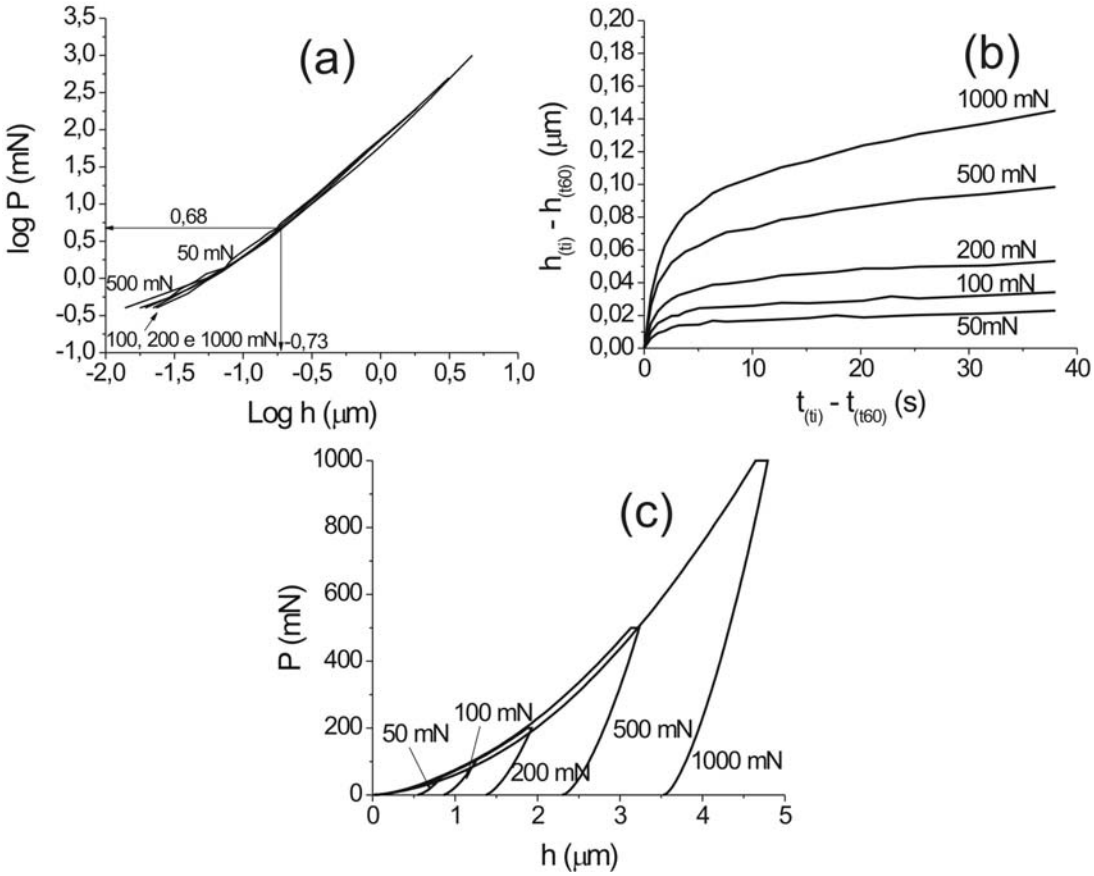

Figure 6 – Nano-indentation Curves for Sample 3 (TMT condition). (a) log(P) *versus* log(h) on loading. (b) Depth Stabilization at maximum load. (c) Load (P) *versus* depth (h).

Table 2 – Values extracted from nano-indentation curves at room temperature.

	Load (mN)	h_{max}^* (μm)	h_f^* (μm)	E_d^*	E_r^*	E_t^*	HV^* average
				(mN.μm)			
Sample 1 AR condtion	50	0.8	0.6	11.2	5.2	16.2	354
	100	1.3	0.9	37.0	16.2	53.3	306
	200	1.8	1.3	98.3	39.2	137.5	295
	500	3.1	2.2	426.7	173.2	600.0	261
	1000	4.5	3.2	1206.3	492.0	1698.8	256
Sample 2 HT condtion	50	0.9	0.6	14.3	4.9	19.2	315
	100	1.3	0.9	41.5	14.7	56.2	286
	200	2.0	1.5	118.4	37.7	156.1	229
	500	3.4	2.6	550.9	147.3	698.3	204
	1000	5.0	3.9	1512.8	405.0	1917.9	190
Sample 3 TMT condtion	50	0.8	0.5	11.4	5.3	16.7	360
	100	1.2	0.9	35.6	15.7	51.3	329
	200	1.9	1.4	108.5	43.8	152.3	269
	500	3.2	2.3	442.0	182.5	624.5	248
	1000	4.8	3.5	1257.8	496.4	1754.2	222

** h_{max} – Indentation depth at maximum load; h_f – Indentation depth after to remove the load; E_d – Dissipation energy; E_r – Recoverable energy; E_t – Total energy; HV – Hardness Vickers.*

4 DISCUSSION

During the application of the load, at nano-indentation test, the samples present two slope regions in the log(P) *versus* log(h) curves, as shown in Figures 4a, 5a and 6a. These regions can be related with the presence of an elastic deformation stage of martensite followed by the martensite variants reorientation stage and the dislocation

generation in the martensitic structure. This behavior is similar to the tensile test for martensitic sample (according to Liu, Li and Ramesh[11]): (i) the first linear region followed by a plateau is related to the elastic zone and martensite variants reorientation (domino detwinning); and (ii) the second linear region is related to the assisted detwinning followed by a dislocation generation region. The Sample 2 (HT condition – Figure 5a) presents a larger dispersion of their log(P) *versus* log(h) curves for different loads, when compared with the Samples 1 (AR condition – Figure 4a) and Sample 3 (TMT condition – Figure 6a). This characteristic is due to a smaller resistance to the penetration (lower Hardness values, HV average), for the Sample 2 (HT condition – Figure 5a), as shown in Table 2.

The maximum load is maintained by an interval of time to evaluate the stabilization of the indentation depth (h) of each sample (Figure 4b, 5b and 6b). After 5 s at maximum load of 50 mN, occurs the stabilization of the indentation depth for all the samples. The stabilization of the indentation depth ($h_{(ti)}$-$h_{(t60)}$), at the maximum load plateau, does not occur for maximum loads greater than 50 mN. However, the increase of the indentation depth ($h_{(ti)}$-$h_{(t60)}$) with elapsing of the time ($t_{(ti)}$-$t_{(t60)}$) is more drastic for loads above 500 mN for the Sample 2 (HT condition – Figure 5b). The nano-indentation curves of P *versus* h (Figure 4c, 5c and 6c) and the Table 2 show that the Sample 1 (AR condition), when compared with a Sample 2 (HT condition) and Sample 3 (TMT condition), has lower indentation depth (h) values at maximum load (h_{max}) and after the removal of the load (h_f). This behaviour is similar for the dissipation and total energies. The Sample 2 (HT condition) dissipates more energy in the martensite variant reorientation and dislocation generation processes when compared with Sample 1 (AR condition) and Sample 3 (TMT condition). This is due to the lower internal stress values or dislocation density resulting from full recrystallization during the thermal treatment at 500ºC for 30 minutes (Sample 2 – HT condition). The recoverable energy during unload step is smaller for Sample 2 than for Sample 1 and Sample 3.

The HV values (average), shown in Table 2 - calculated from nano-indentation test curves, decrease with the increase of the applied maximum load. In the nano-indentation test, the load is increased incrementally until a maximum value is reached, independent of the answer to the material deformation, and the hardness (HV) is the relation between the maximum load and the contact area of indenter with the sample before the unloading. This means that, increasing the applied maximum load does not imply a proportional increase of the area of contact of the indenter/sample, but the rate of increase of the contact area is bigger than the increase of the load. This behaviour should be associated to the mechanism of deformation of the martensite associated to the detwinning, which occurs with an increase of the extension without increase of the applied load. This behaviour is evidenced in Figure 4b, 5b and 6b by the indentation depth stabilization for loads lower or equal to 200 mN (initial domino detwinning process) and continuous increase of the indentation depth for maximum loads equal or higher than 500 mN (stage with large deformations related with assisted detwinning). The Sample 1 and Sample 3 present higher hardness values (HV average) than the Sample 2.

5 SUMMARY

Nano-indentation tests, for the Ni-Ti alloy at different conditions under study, showed clearly that:

- Martensite variant reorientation related with domino detwinning occurs at low indenter load;
- The maximum load used (1000 mN) and creep time (60 s) is not enough for the stabilization of the indentation depth related with dislocation generation;
- Mechanical properties change by dissipation and recoverable energies.

Acknowledgments

The authors wish to acknowledge the financial support from FCT/MCTES for the pluriannual funding of CENIMAT and Valdemar Fernandes for the nano-indentation tests and calculations.

REFERENCES

1 WASILEWSKI, R.J., BUTLER, S.R., HANLON, J.E., WORDEN, D., Homogeneity Range and Martensitic Transformation in TiNi, Metallurgical Transactions, v. 2, p. 229, 1971.

2 KHACHIN, V.N., PASKAL YU, I., GUNTER, V.E., MONASEVICH, A.A., SIVOKHA, V.P., Fizika Metallov i Metallovedenie, v. 46, p. 511, 1978.

3 LIU, Y., CHEN, X., McCORMICK, P.G., Effect of Low Temperature Ageing on the Transformation Behaviour of Near-equiatomic NiTi, Journal of Materials Science, v. 32, p. 5979, 1997.

4 SOMSEN, Ch., ZÄHRES, H., KÄSTNER, J., WASSERMANN, E.F., KAKESHITA, T., SABURI, T., Influence of Thermal Annealing on the Martensitic Transitions in Ni-Ti Shape Memory Alloys, Materials Science and Engineering A, v. 273-275, p. 310, 1999.

5 MILLER, D.A., LAGOUDAS, D.C., Influence of Cold Work and Heat Treatment on the Shape Memory Effect and Plastic Strain Development of NiTi, Materials Science and Engineering A, v. 308, p. 161, 2001.

6 FILIP, P., MAZANEC, K., On Precipitation Kinetics in TiNi Shape Memory Alloys, Scripta Materialia, v. 45, p. 701, 2001.

7 Antunes, J.M., Cavaleiro, A., Menezes, L.F., Simões, M.I., Fernandes, J.V., Ultra-microhardness Testing Procedure with Vicker Indenter, Surface and Coatings Technology, v. 149, p. 27, 2002.

8 Gall, K., Juntunen, K., Maier, H.J., Sehitoglu, H., Chumlyakov, Y.I., Instrumented Micro-indentation of NiTi Shape Memory Alloys, Acta Materialia, v. 49, p. 3205, 2001.

9 BRAZ FERNANDES, F.M., PAULA, A.S., CANEJO, J.P.H.G., MAHESH, K.K., SILVA, R.J.C., Kinetics Characterization of Martensitic Transformation on Ti-Rich Ni-Ti SMA, Proceedings of SMST2004: International Conference on Shape Memory and Superelastic Technologies, p. 51, Editor Mathias Mertmann, ASM, Ohio, 2006.

10 PAULA. A.S., Tratamentos Termomecânicos de Ligas do Sistema Ni-Ti: Caracterização Estrutural e Optimização das Propriedades Associadas ao Efeito de Memória de Forma, PhD Thesis, FCT/UNL, Lisbon – Portugal, 2006.

11 Liu, Y., Li, Y., Ramesh, K.T., Rate Dependence of Deformation Mechanisms in a Shape Memory Alloy, Philosophical Magazine A, v. 82, p. 2461, 2002.